

Thermal Conductivity of Double-Nitrate Crystals below 1°K*

J. E. ROBICHAUX AND A. C. ANDERSON

Department of Physics and Materials Research Laboratory, University of Illinois, Urbana, Illinois 61801

(Received 11 June 1970)

The thermal conductivities of high-purity cerium magnesium nitrate and lanthanum magnesium nitrate single crystals have been measured in zero or small magnetic fields. The phonon mean free path is found to be limited by processes intrinsic to the crystal. This mean free path can be longer than nominally allowed by the dimensions of the specimen. Measurements were also made on samples doped with other rare-earth ions. The resonant absorption of phonons by the non-Kramers ions Pr and Ho is observed and is shown to result from electronic transitions between hyperfine energy levels.

I. INTRODUCTION

The double nitrates, in particular, lanthanum magnesium nitrate (LMN) and cerium magnesium nitrate (CMN),¹ have been the subject of a great deal of experimental work. Since magnetic ions can be substituted in various concentrations in either the La or the Mg sites in the nonmagnetic host LMN, this crystal has provided numerous systems for magnetic-resonance studies. CMN, being a highly dilute paramagnet which obeys the Curie law down to $\sim 0.005^\circ\text{K}$, is of current importance in both the production and the measurement of very low temperatures.

Nevertheless, in spite of the extensive work on these crystals, their properties below $\sim 1^\circ\text{K}$ are not well understood. As an example, magnetic relaxation data on CMN obtained above 1°K cannot be extrapolated to explain the low-temperature relaxation behavior in small magnetic fields. Even the specific heat of CMN calculated theoretically has only recently approached quantitative agreement with the values obtained experimentally at very low temperatures.² We therefore have undertaken a systematic study of the low-temperature properties of the double nitrates. In the present paper we report on measurements of the thermal conductivity of both pure and doped single crystals of LMN and CMN in magnetic fields of 0–240 G. The purpose of this work was to obtain an understanding of phonon transport. For all the samples studied we have found (a) that the phonon mean free path is limited internally, and (b) that the thermal phonons are resonantly “scattered” by hyperfine transitions on certain rare-earth impurities.

II. TECHNIQUE

The LMN and CMN crystals were grown on Teflon flats by desiccating a saturated aqueous solution at a temperature of 0°C , the starting material being of the highest available purity.³ In the case of CMN the material was also doubly recrystallized. When doping with other rare earths, the concentration grown into the crystal was always less than the concentration in solution. The ratio of these concentrations, though constant for a given ion, decreased as

the mass of the rare-earth ion increased, becoming $\approx 1/300$ for Ho.

The crystals used were generally transparent and optically perfect, even though it was determined empirically that, in the temperature range of interest, regions of translucency did not affect their thermal conductivity. The natural shape of the double nitrate crystal is a flat, essentially hexagonal plate with a thickness-to-“diameter” ratio of $\sim 1/10$. Samples, typically of 1 cm width and 2.5–4.5 cm length, were cut from these crystals using a wet-string saw and then mounted as shown in Fig. 1. The upper resistance thermometer⁴ was uncalibrated and served, by means of electronic control of the dilution refrigerator, to maintain that point on the crystal which was in contact with the thermometer at a constant temperature during a measurement. The lower resistance thermometer was used to measure both the temperature T in the absence of a thermal flux and the temperature difference ΔT in the presence of a thermal flux. This lower thermometer was calibrated to an accuracy of better than 1% against a single-crystal sphere of CMN, which in turn was calibrated against the vapor pressure of liquid He³. Usually $\Delta T/T \lesssim 0.1$, resulting in a random error of $\sim \pm 3\%$. The largest systematic error in our values of thermal conductivity arose from the measurement of the dimensional ratio of the sample, primarily because of the finite width of the thermometers. This error could be $\lesssim 10\%$ and is, of course, temperature independent.

In the naive expectation that a knowledge of sound velocities would assist in understanding the transport properties, we measured the transverse wave velocity in CMN over the frequency range $(3-30) \times 10^6 \text{ Hz}$ ⁵ using Y -cut quartz transducers bonded with phenyl salicylate. The measurements were made at a temperature of $\sim 0^\circ\text{C}$ since this improved the bond. The velocity parallel to the hexagonal axis was measured in two samples, of similar thickness, and found to be $v(0)_m = 4 \times 10^4 \text{ cm/sec}$, independent of the transducer used or of its orientation on the surface as would be expected. The velocity was also measured perpendicular to the hexagonal axis on two samples, differing in length by a factor of 2.5, and found to be $v(\pi/2)_m = 1.3 \times 10^5 \text{ cm/sec}$. This velocity was independent of

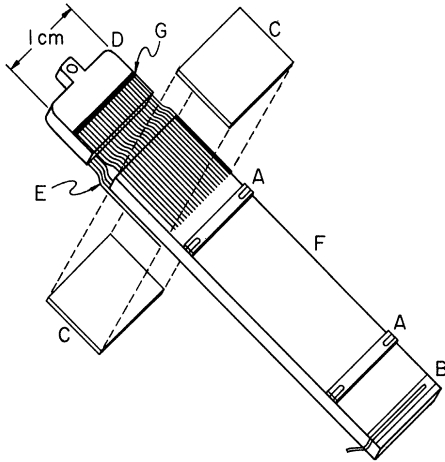


FIG. 1. Technique used to mount the double nitrate crystals (F) for thermal conductivity measurements. The fan of loose wires (E), which was In soldered (G) to the copper mount (D), was thermally bonded to the crystal using Apiezon *N* grease. The wires were held in position by lashing pieces C together with thread, as indicated. The resistance thermometers are at A, and the electrical heater at B. The separation between the thermometers and the wires or heater was always greater than $1.5t$, t being the thickness of the samples.

the direction of propagation in the (001) crystal plane, and also was *independent* of the orientation of the transducer on the crystal surface. A ratio $v(\frac{1}{2}\pi)/v(0) > 1$ would be expected for CMN, but $v(\frac{1}{2}\pi)$ should depend on the transducer orientation. That is, a slow as well as a fast shear mode should have been detected.⁶ We have no explanation for this result. Since only about three echoes were observed in every case, and these were rather wide, the error in the above values is estimated at $\sim \pm 20\%$. Accurate measurements of sound velocities at $\sim 300^\circ\text{K}$ in plastics, metals, and other crystals may be obtained with ease relative to such measurements on CMN. Nevertheless, we were reasonably convinced that echoes were being observed.

The sound velocities at low temperature will be larger than the values measured at room temperature. Since the lattice parameter parallel to the hexagonal axis decreases by 1.7% between room temperature and 4°K , versus 0.5% perpendicular to this axis,⁷ $v(0)$ will increase the greater amount. This will reduce the anisotropy, i.e., the ratio of $v(\frac{1}{2}\pi)/v(0)$, from its room-temperature value of 3.25.

III. RESULTS AND ANALYSIS

A. "Pure" CMN and LMN

Figure 2 shows the results of the thermal-conductivity measurements on two samples of "pure," i.e., not intentionally doped, CMN and LMN cut such that the thermal gradient was perpendicular to the hexa-

gonal axis. The impurity analyses of the crystals themselves, obtained by mass and emission spectroscopy, are given in Table I and are considerably more conservative than the specifications provided with the starting materials. The thermal conductivity of all samples had a temperature dependence lying between $T^{2.8}$ and $T^{3.0}$. A power less than 3.0 suggests specular reflection of phonons from the crystal surface, but "sand blasting"⁸ the surfaces made no significant change in the conductivity. Several samples were reduced in thickness, but again there was no systematic change in the thermal conductivity. The implication is therefore that the dominant phonon scattering mechanism is internal to the crystal and is nearly frequency independent. In most samples the temperature dependence decreased near 1°K , as for the CMN sample of Fig. 2. Since the Debye Θ for LMN and CMN is $\sim 70^\circ\text{K}$, this decrease may indicate the approach to the maximum in the thermal conductivity. The deviation does not have the proper temperature dependence to be caused by the scattering of phonons from point defects or dislocations.

The results of Fig. 2 may be compared with a theoretical calculation of the thermal conductivity. Since the lattice specific heats of CMN and LMN

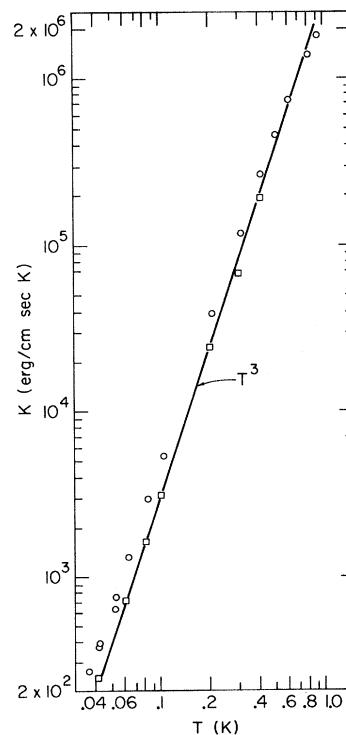


FIG. 2. Thermal conductivity versus temperature for "pure" LMN (\square) and CMN (\circ) measured in a direction perpendicular to the hexagonal axis.

vary essentially as T^3 near 1°K ,^{9,10} a Debye model is appropriate. We first compute the specific heat from our measured sound velocities to provide a comparison with the measured (lattice) specific heat C_m of LMN or CMN, namely, $C_m \simeq (1.2 \times 10^{29} \text{K}^{-3}) T^3 \text{ erg}/^\circ\text{K cm}^3$.^{9,10} Assuming the contribution from dilatational modes is negligible, one obtains in the limit of low temperatures

$$C = 4.1 \times 10^{17} T^3 \iint 2d\Omega / 4\pi [v(\theta)]^3. \quad (1)$$

Here, to be consistent with our sound-velocity measurements of Sec. II, the transverse modes are assumed to have the same velocity $v(\theta)$. The angle θ is measured from the hexagonal axis. Hence, for these hexagonal crystals¹¹

$$v(\theta)^{-1} = A + B \sin^2\theta + D \sin^2\theta \cos^2\theta. \quad (2)$$

Letting $D=0$, since we have measured only $v(0)_m$ and $v(\frac{1}{2}\pi)_m$, Eq. (1) becomes $C = (4.2 \times 10^{29} \text{K}^{-3}) T^3 \text{ erg}/^\circ\text{K cm}^3$, a factor of 35 larger than the measured specific heat C_m . Even if one takes into consideration the increase in v with decreasing temperature and that D in Eq. (2) is finite, it must be concluded that our measurements of v at 273°K are not indicative of the low-temperature values. We therefore deduce an average velocity $\bar{v} \simeq 1.9 \times 10^6 \text{ cm/sec}$ from the measured heat capacity and also assume, lacking any other evidence, that $v(\frac{1}{2}\pi)/v(0) \lesssim 3$ from the high-temperature measurements of the sound velocity.

The thermal-conductivity tensor may be written, in the notation of Carruthers,¹²

$$K_{ij} = \frac{1}{(2\pi)^3} \sum_{\alpha} \iiint q^2 dq d\Omega \tau_{\alpha}(q) C(\omega) (v_{\alpha})_i (v_{\alpha})_j. \quad (3)$$

This expression may be rewritten to allow the inclusion of the measured specific heat C_m in the form

$$K_{ii} = [C_m(\bar{v})^3] \iint \frac{\lambda(\theta) [v(\theta)]^2 d\Omega}{4\pi v(\theta)^4} \quad (4)$$

for the usual case in which the temperature gradient is measured in the direction of the thermal flux. In arriving at Eq. (4) it has been assumed that the

TABLE I. Impurity content of the "pure" CMN and LMN crystals, given in ppm, atomic, relative to the Ce or La, respectively.

CMN		LMN	
Pr	5	Eu	100
La	6	Pr	5
		Ce	70
Cu	70	Cu	100
Ni	40	Ni	100
Fe	20	Fe	100
Mn	20	Mn	100
Cr	100	Cr	600
V	80	V	200

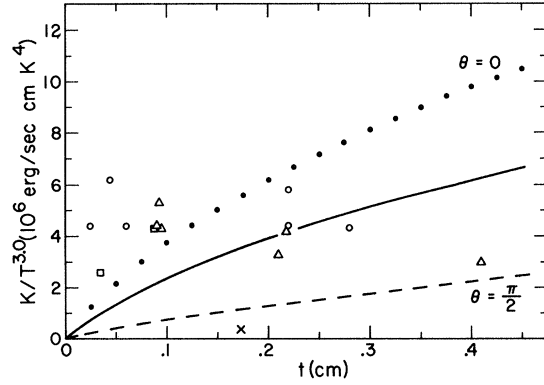


FIG. 3. The averaged value of K/T^3 , obtained for each individual sample, versus thickness for samples of 1.0-cm width. The data are for pure CMN (\circ), pure LMN (\square), as well as doped crystals (\triangle), all measured at $\theta = \frac{1}{2}\pi$. One sample of CMN is shown (\times) which was measured at $(\theta=0)$. The fact that some of the data were divided by $T^{3.0}$ rather than $T^{2.8}$ does not alter significantly the appearance of this plot. The solid line is calculated for the case of an isotropic velocity. The other two curves are calculated for an anisotropy of $v(\frac{1}{2}\pi)/v(0) = 3.2$, as explained in the text. The dashed line is for the anisotropic conductivity measured perpendicular ($\theta = \frac{1}{2}\pi$) to the crystallographic hexagonal axis, and the dotted line is for the case parallel ($\theta=0$) to this axis.

phonon relaxation time τ is independent of frequency ω , that $\lambda(\theta) = v(\theta)\tau(\theta)$, and that only the two degenerate transverse modes need to be considered. For a long slab of width w and thickness t , Eq. (4) becomes, in the limit of diffuse scattering of phonons at the boundaries,

$$K\left(\frac{\pi}{2}\right) = \frac{1}{3} C_m \frac{(\bar{v})^3}{[v(\frac{1}{2}\pi)]^2} \left\{ \frac{3}{4} t \ln \left[\frac{w}{t} + \left(1 + \left(\frac{w}{t} \right)^2 \right)^{1/2} \right] + \frac{3}{4} w \left(1 + \frac{1}{4} B \right) \ln \left[\frac{t}{w} + \left(1 + \left(\frac{t}{w} \right)^2 \right)^{1/2} \right] \right\} \quad (5a)$$

or

$$K(0) = \frac{1}{3} C_m \frac{(\bar{v})^3}{[v(\frac{1}{2}\pi)]^2} \left\{ \frac{3}{4} t \left(1 + \frac{3}{4} B \right) \ln \left[\frac{w}{t} + \left(1 + \left(\frac{w}{t} \right)^2 \right)^{1/2} \right] + \frac{3}{4} w \left(1 + \frac{3}{4} B \right) \ln \left[\frac{t}{w} + \left(1 + \left(\frac{t}{w} \right)^2 \right)^{1/2} \right] \right\} \quad (5b)$$

for the conductivity perpendicular to or parallel to the crystallographic hexagonal axis, respectively. Here $B = [v(\frac{1}{2}\pi)/v(0)]^2 - 1$ and is zero for an isotropic material for which $v(0) = v(\frac{1}{2}\pi) = \bar{v}$. If Eq. (5) is evaluated for both the isotropic case and for $v(\frac{1}{2}\pi)/v(0) = 3.2$, the curves of Fig. 3 are obtained for samples of width 1.0 cm and of the indicated thicknesses. Also plotted on Fig. 3 are the average, for each sample, of the measured K/T^3 values for fourteen samples for which the thermal conductivity

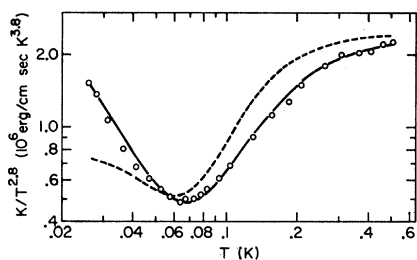


FIG. 4. Thermal conductivity data, divided by $T^{2.8}$, for a sample of CMN doped with 0.8 at. % Pr. The solid curve is a theoretical fit to these data using the asymmetric line shape shown in Fig. 6(iii), as explained in the text. The broken curve is a theoretical fit using a symmetric line shape, in this case a Lorentzian.

was measured perpendicular to the hexagonal axis. These data should fall on or below the dashed curve if the double nitrates are highly anisotropic, or on or below the solid line if the materials are isotropic. The fact that K/T^3 is independent of thickness and surface conditions is indicative of a frequency-independent, internal phonon scattering process as mentioned before. On the other hand the fact that the data fall *above* the respective curves in Fig. 3 means that the effective phonon mean free path is larger than nominally permitted by the physical geometry of the sample.

The thermal conductivity of CMN *parallel* to the hexagonal axis was measured in one sample, since only one optically perfect crystal was available of sufficient size. The average value of K/T^3 for this sample is included in Fig. 3. In this case the conductivity is very small relative to the dotted curve (anisotropic case) or solid curve (isotropic case). To learn if boundary scattering of phonons was important, the thickness was reduced by a factor of 2. The conductivity, rather than being decreased by a factor of ~ 2 , was instead decreased by a factor of ~ 9 . (Here it should be noted that the thermal conductivity for this sample, as well as for all others, did reproduce with thermal cycling.) In view of this large decrease in conductivity, it was thought that some physical damage may have been done in reducing the sample thickness, since in this case the cleavage plane was perpendicular to the long dimension of the crystal. The crystal was therefore placed in a sealed enclosure and "annealed" for one week at a temperature of 60°C . This treatment reduced the thermal conductivity by another factor of ~ 30 . After annealing, several planes perpendicular to the hexagonal axis could be observed by transmitted light. When stressed, the sample parted along these planes.

The internal, frequency-independent phonon scattering is quite likely occurring at lattice imperfections having dimensions greater than the phonon wavelength

and lying in the (001) crystal planes, since the crystal is most easily damaged physically in this cleavage plane, as has been observed visually as well as by x-ray⁷ and magnetic¹³ techniques. This suggestion is reinforced by the results obtained with the CMN sample used to measure thermal conductivity parallel to the hexagonal axis. The imperfections, however, must be grown into the crystal since (with the one exception noted in the previous sentence) neither handling nor thermal cycling significantly changed their thermal conductivity. The cloudiness occasionally found in double-nitrate crystals results when the (001) planes nucleate at several points and then grow together to trap "bubbles" of liquid. Under slower growing conditions the "bubbles" are not visible, but presumably the condition is not absent. The question of whether twinning, of a type in which one (001) plane is rotated $\approx 30^\circ$ relative to a neighboring plane, is possible in this not-quite-hexagonal crystal¹⁴ cannot be answered here. There are some general similarities between the measurements on the double nitrates and on graphite, another hexagonal crystal with weak coupling between (001) planes,¹⁵ but these do not serve to clarify the situation.

It was noted above that if one chooses to talk in terms of a phonon mean free path, the deduced mean free path for a measurement made perpendicular to the hexagonal axis is considerably larger than one limited by the sample dimensions. Phonon focusing is present in these crystals,¹⁶ but it seems more likely that the long mean free path results from specular reflection, either partial or total, from (001) planes which contain grown-in planar defects. This would be consistent with the frequently observed $T^{2.3}$ temperature dependence and with the short mean free paths deduced from measurements made in a direction parallel to the hexagonal axis. One might note that there would not be an anomalously long phonon mean free path if the measured values of sound velocity (Sec. II) had been used to calculate the thermal conductivity. However, if these values of sound velocity are to be used, one is then faced with a large discrepancy between the measured and

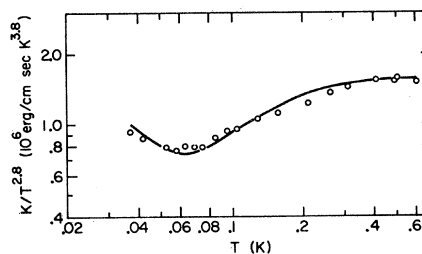


FIG. 5. Thermal-conductivity data, divided by $T^{2.8}$, for a sample of CMN doped with 0.18 at. % Pr. The solid curve is a theoretical fit to the data.

calculated values of the lattice heat capacity. The lattice heat capacity has been shown to vary as $\sim T^3$ down to 2°K ,⁹ and the thermal conductivity is here shown to vary as T^3 from 0.04 to 1°K . Although these two measurements do not overlap, they nevertheless make it unreasonable to expect a large dispersion in phonon velocity near 1°K . Rather it would appear that our room-temperature velocity measurements either are not applicable or are simply erroneous.

An anomalous contribution to the heat capacity of certain CMN samples has been reported in the temperature range ~ 0.01 – 0.5°K .¹⁰ In view of the T^3 temperature dependence observed for the thermal conductivity between 0.04 and 1°K , it is highly unlikely that the anomalous heat capacity is inherently associated with the lattice either in the form of a phonon dispersion or of localized phonon states.

B. Doped Samples

In Figs. 4 and 5 are shown the thermal conductivity data for CMN samples doped with 0.8 and 0.18 at. % Pr, respectively. Since all doped samples of CMN had temperature dependencies near $T^{2.8}$, the data of Figs. 4 and 5 have been divided by $T^{2.8}$ to remove most of the temperature dependence. A depression in the conductivity near 0.06°K is readily apparent. The magnitude and shape of this depression was

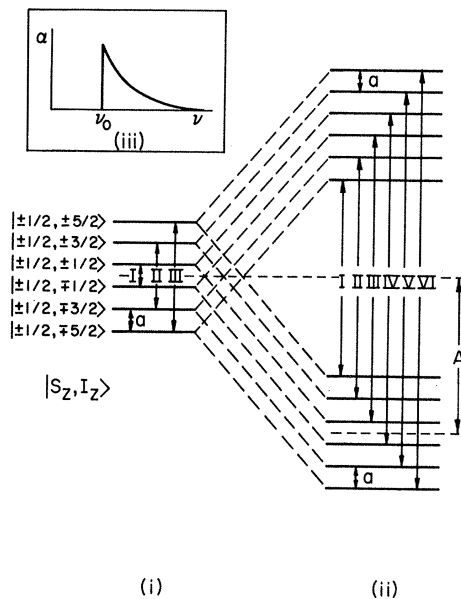


FIG. 6. A possible energy-level scheme for Pr^{3+} in CMN. In (i) the electronic levels are split only by the nuclear magnetic hyperfine field, the separation between levels being a . For comparison, in (ii) the levels are shown for the case of a large, externally applied magnetic field proportional to A , as in the case of paramagnetic resonance. In (iii) the line shape for any of the indicated transitions is shown schematically, where ν is the phonon frequency and $\nu_0 = ah/h$.

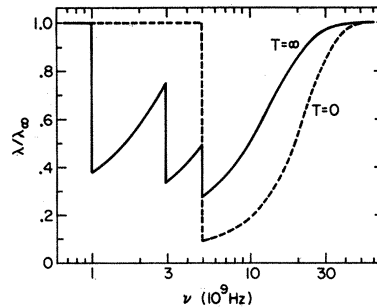


FIG. 7. The phonon free path λ , normalized to a value of unity at very high frequencies, plotted against frequency for the sample of Fig. 4. The solid line is the phonon free path for high temperatures, i.e., with the energy levels of Fig. 6(i) equally populated, while the broken line is for the case of very low temperatures.

independent of a magnetic field of 240 G applied either parallel or perpendicular to the hexagonal axis of the crystals.

It is suggested that this behavior results from the resonant "scattering" (i.e., absorption and reemission) of phonons by electronic transitions between hyperfine levels of the Pr^{3+} impurity. A possible energy-level structure for the Pr ion is shown in Fig. 6, together with the line shape expected from the combined effects of electric coupling to the phonon field and broadening due to the strained lattice around the Pr sites.¹⁷⁻¹⁹ Also shown for comparison is the more familiar level structure observed in large external magnetic fields as in EPR experiments.

Numerous experimental and theoretical publications have dealt with the resonant scattering of phonons by magnetic ions,²⁰⁻²⁹ a phenomenon which is related to the field of acoustic paramagnetic resonance.^{30,31} This previous work was generally concerned with transport behavior in large applied magnetic fields. In the present work, however, there is no applied field and thus the energy splittings are caused predominantly by the magnetic field produced by the ^{141}Pr nucleus.

Equation (3) is appropriate to a calculation of the thermal conductivity where τ is frequency dependent. If, for simplicity, it is assumed that both τ and ν are isotropic and that the phonon spectrum is Debye-like, Eq. (3) becomes

$$K = \frac{k}{3\pi^2(\bar{v})^2} \left(\frac{kT}{\hbar} \right)^3 \int \frac{x^4 \lambda(x) e^x dx}{(e^x - 1)^2}, \quad (6)$$

where $x = \hbar\nu/kT$. The three electronic transitions which are possible for the Pr ion are shown schematically as I, II, and III in Fig. 6(i), each having the line shape of Fig. 6(iii). This line shape has, for electrically induced transitions, the form $\exp[d(\nu_0 - \nu)/\nu_0]$ for $\nu \geq \nu_0$ and zero for $\nu < \nu_0$, where ν_0 is the frequency for resonant absorption in the absence of lattice

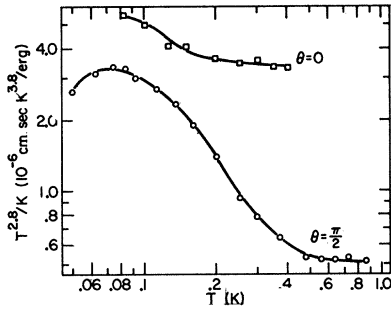


FIG. 8. Thermal resistivity data, multiplied by $T^{2.8}$, for two samples of CMN each containing ~ 1 at. % Pr, one (O) measured perpendicular to the hexagonal axis ($\theta = \frac{3}{4}\pi$), the other (□) parallel to the hexagonal axis ($\theta = 0$). The solid curves are only to assist in visualizing the data. The increase in thermal resistance in both crystallographic directions due to the Pr impurity is readily apparent.

strain.¹⁷⁻¹⁹ However as the temperature is reduced the upper levels depopulate so that, as $T \rightarrow 0$, only transition III can be excited. Assuming the additivity of phonon relaxation rates τ^{-1} this information can be written, in an approximate manner, into a frequency-dependent phonon free path of the form

$$\lambda(\nu)^{-1} = \frac{T^{0.2}}{b} + \frac{c}{z} \exp\left(\frac{-2a}{T} + \frac{d(\nu_0 - \nu)}{\nu_0}\right)_{\nu \geq \nu_0} + \frac{c}{z} \exp\left(\frac{-a}{T} + \frac{d(\nu_0 - \nu)}{3\nu_0}\right)_{\nu \geq 3\nu_0} + \frac{c}{z} \exp\left(\frac{d(\nu_0 - \nu)}{5\nu_0}\right)_{\nu \geq 5\nu_0}, \quad (7)$$

where

$$z = \sum_{i=0}^5 \exp(-ia/T) \quad \text{and} \quad \nu_0 = ak/h.$$

The first term is related to the internal scattering discussed in Sec. II A. The $T^{0.2}$ has been inserted to match the data in the nonresonant regime to the theoretical expression of Eq. (6). The other terms represent the resonant scattering mechanism and are zero for $\nu < \nu_0$, $\nu < 3\nu_0$, and $\nu < 5\nu_0$, respectively. The use of an isotropic cross section in these terms does not significantly change the temperature dependence of the computed conductivity.

The solid curves of Figs. 4 and 5 were obtained by substitution of Eq. (7) into Eq. (6) and varying the parameters a , b , c , and d to obtain the best fit to the data. In both cases $a = 0.048^\circ\text{K}$. This value of the hyperfine interaction constant may be compared to a value of $a = 0.055^\circ\text{K}$ obtained by magnetic resonance in large magnetic fields.^{17,19} If an additional symmetrical linewidth due to the dipolar magnetic fields from the Ce^{3+} were to be introduced into the calculation, the

agreement with the magnetic-resonance data could be improved. The width required by these fits, namely, $d = 0.8$, is rather large for the Pr concentration. In LMN, in large magnetic fields, it is necessary to increase the concentration to $\approx 10\%$ to obtain a similar width for rf induced transitions.¹⁹ The net free path versus frequency for the sample of Fig. 4 is shown in Fig. 7, where the small temperature dependence of $T^{0.2}$ [Eq. (7)] has been omitted without compromising the essential features of the plot.

The ratio of the concentration dependent term c for the two crystals is ~ 3 , as compared to the measured concentration ratio of 5. A somewhat better agreement could be obtained by using different width parameters d for the two samples; however the credibility of the data or of the approximate model is not thereby enhanced.

The data of Figs. 4 and 5 cannot be fitted using a more symmetrical absorption curve such as a Gaussian, a Lorentzian, or some *ad hoc* curve.²⁵ An attempt to fit a Lorentzian is shown by the broken line in Fig. 4. Improving the fit at high temperatures only worsens the low-temperature fit.

The thermal resistivities of two CMN crystals having the same concentration of $\sim 1\%$ Pr are shown in Fig. 8. In one case the resistivity was measured parallel to the hexagonal axis ($\theta = 0$), and in the other case the measurements were made perpendicular to this axis ($\theta = \frac{1}{2}\pi$). Writing the cross section for resonant absorption of phonons as³² $\sigma = \sigma_0 \sin^2\theta$, the net phonon free path λ can be approximated by

$$\lambda^{-1} = N \sin^2\theta + M \quad (8)$$

near the frequency of the resonance. Again this is a simplification since, for example, the strain field distortion of the electronic state will tend to reduce the anisotropy of Eq. (8). Nevertheless, if the magnitude of M for each sample of Fig. 8 is established near 1°K where $N = 0$,³³ a value of N near the resonance can be deduced. For an isotropic velocity the ratio of the value of N for one crystal, divided by the value of N obtained for the other crystal, is 1.7. This ratio is an upper limit and would be reduced if the anisotropy of Eq. (8) were reduced. Since the Pr concentration in the two crystals is the same, the ratio should be unity. The lack of quantitative agreement with the deduced ratios is not unreasonable in view of the approximations made in the computation. The qualitative result is that one does and should observe a significant depression in the thermal conductivity even in a direction in which the resonant absorption cross section is ~ 0 .

From hyperfine splittings observed in magnetic-resonance measurements on ^{143}Nd and ^{145}Nd in LMN,¹⁸ one would expect a depression centered near 0.03°K in the thermal conductivity of a sample suitably doped

with Nd. However, with a concentration of 15% Nd no indication of a resonant absorption was observed in LMN down to 0.04°K. A resonance may lie below this temperature, but more likely the lack of an effect is due to the fact that Nd³⁺ is a Kramers ion and hence interacts much less strongly with lattice waves than the Pr³⁺ ion.

Ho³⁺ and Tb³⁺ are both non-Kramers ions which exhibit large hyperfine splittings in many environments.³⁴ As mentioned in Sec. II however, Tb and Ho, being at the more massive end of the rare-earth series, are preferentially excluded during crystallization of the double nitrates. This indicates that the ions do not fit well into the lattice, and as a consequence the electronic ground state is uncertain. Thus one cannot predict the temperature at which resonant scattering might occur in double nitrate samples doped with these ions. The results for ≈ 10 at. % Tb and ≈ 0.2 at. % Ho in LMN are shown in Fig. 9. For Tb there is no resonant depression observed. For Ho the high-temperature extremity of a resonance is detected, giving a hyperfine interaction parameter of $a \lesssim 0.02^\circ\text{K}$.

Crystals containing ions such as Pr should exhibit a Schottky-type heat capacity if the hyperfine splitting of the ground state is that shown in Fig. 6(i). This would not be the usual Schottky peak since in the present case the energy levels are not discrete, but rather "smeared out" owing to the strain fields at the ion sites. As a result, the modified Schottky peak is broadened toward higher temperatures and reduced in height at the maximum. The magnetic specific heat of 100% Pr double nitrate has been measured at temperatures above 2°K, and the high-temperature tail of a Schottky peak is observed.³⁵ If one assumes the zero-field hyperfine splitting of Fig. 6(i) with $a=0.05^\circ\text{K}$, the calculated magnetic heat capacity is an order of magnitude too small, even using the modified Schottky peak mentioned above. The problem is quite likely associated with the fact that the magnetic resonance line shape is a function of Pr concentration. With 100% Pr content, the line shape is symmetrical with a half-width at half-maximum of 0.14°K.¹⁹ If one assumes the width to result from an effective interaction³⁶ which is also present in zero applied field,³⁷ the zero-field energy-level scheme is very roughly depicted by Fig. 6(ii) with $A \approx 0.3^\circ\text{K}$ (but with the individual levels very broad compared to $a=0.05^\circ\text{K}$). This is in fair agreement with the value $A=0.23^\circ\text{K}$ obtained from the specific-heat data.³⁵ Hence the shape of a plot of specific heat versus temperature for Pr in the double nitrates would depend critically on the Pr content.

In crystals such as Pr double nitrate, where the coupling between spin and phonon systems is large, some frequency dispersion of the phonon velocity should occur. The influence of this effect on the thermal conductivity near the spin-phonon resonance is rather

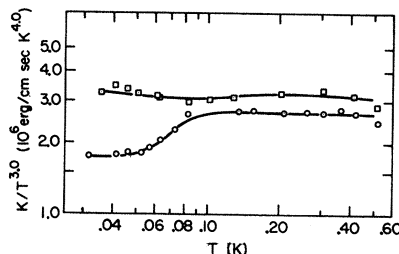


FIG. 9. Thermal-conductivity data divided by T^3 for LMN doped with 10 at. % Tb (\square) or 0.2 at. % Ho (\circ), versus the temperature T . A depression resulting from the resonant absorption of phonons by Ho ions is observed.

small²⁰ and cannot be resolved in the present experiments. Phonons also may be scattered by spin fluctuations even at frequencies well above a resonance.²¹ In the present work, owing to the lack of reproducibility from sample to sample as seen in Fig. 3, it can only be stated that there is no evidence of an appreciable difference in the thermal conductivity (well removed from a resonance, if one exists) between samples which contain paramagnetic ions and those samples which are nonmagnetic.

IV. SUMMARY

The thermal conductivity of pure CMN or LMN was found to be independent of the size and surface condition of the sample. The thermal conductivity was also anisotropic, being larger in the direction perpendicular to the crystalline hexagonal axis. The phonon mean free path deduced from the conductivity measured perpendicular to the hexagonal axis was essentially independent of frequency and larger than the thickness of the sample. All these observations are consistent with the suggestion that specular phonon scattering occurs at defects with the sample, these extended defects lying in planes having normals parallel to the hexagonal axis. Independent observations which support this suggestion have been presented. The results cannot be explained simply in terms of the anisotropy of the crystal.

Thermal conductivity measurements from LMN or CMN samples doped with the non-Kramers ions Pr or Ho exhibited a depression near $\approx 0.05^\circ\text{K}$ which was independent of magnetic fields up to 240 G. For Pr this depression could be explained by the process of resonant scattering of phonons by electronic transitions between hyperfine levels of the Pr³⁺ ion. The level splittings and nonsymmetrical line shapes required to fit the thermal-conductivity data are very similar to the EPR spectra observed for Pr in LMN in large magnetic fields.

ACKNOWLEDGMENT

The authors thank Professor H. J. Stapleton for several informative discussions on the double nitrates.

* Work supported in part by the Advanced Research Projects Agency under Contract No. HC 15-67-C-0221. It is being submitted by J. E. Robichaux in partial fulfillment of the Ph.D. degree at the University of Illinois.

¹ LMN and CMN are, respectively, $[\text{La}(\text{NO}_3)_6]_2[\text{Mg}(\text{H}_2\text{O})_6]_3 \cdot 6\text{H}_2\text{O}$ and $[\text{Ce}(\text{NO}_3)_6]_2[\text{Mg}(\text{H}_2\text{O})_6]_3 \cdot 6\text{H}_2\text{O}$.

² R. P. Hudson, *Cryogenics* **9**, 76 (1969).

³ The rare-earth nitrates were obtained from American Potash and Chemical Corp., Rare-Earth Division, West Chicago, Ill. The cerous nitrate was labeled as 99.9999% pure, the lanthanum nitrate as 99.999% pure. The magnesium nitrate was obtained from Mallinckrodt Chemical Works, St. Louis, Mo.

⁴ J. E. Robichaux and A. C. Anderson, *Rev. Sci. Instr.* **40**, 1512 (1969).

⁵ The measurements were obtained with a model-6000 pulse generator and receiver with model-950 plug-in, manufactured by Matex Inc., Providence, R.I.

⁶ See, for example, M. J. P. Musgrave, *Proc. Roy. Soc. (London)* **A226**, 356 (1954).

⁷ D. Schiferl, *J. Chem. Phys.* **52**, 3234 (1970).

⁸ The "sand blasting" was done with 27- μ aluminum oxide powder.

⁹ C. A. Bailey, *Proc. Phys. Soc. (London)* **83**, 369 (1964). We assume for CMN a density of 2.0 g/cm³ and a molecular weight of 765 g/ion.

¹⁰ R. P. Hudson and R. S. Kaeser, *Physics* **3**, 95 (1967).

¹¹ E. Schmid and W. Boas, *Plasticity of Crystals* (Chapman and Hall, London, 1968), Chap. 1, p. 21.

¹² See, for example, P. Carruthers, *Rev. Mod. Phys.* **33**, 92 (1961).

¹³ S. J. Williamson, H. C. Praddaude, R. F. O'Brien, and S. Foner, *Phys. Rev.* **181**, 642 (1969). See also P. L. Scott, H. J. Stapleton, and C. Wainstein, *ibid.* **137**, A71 (1965).

¹⁴ A. Zalkin, J. D. Forrester, and D. H. Templeton, *J. Chem. Phys.* **39**, 2881 (1963).

¹⁵ C. A. Klein and M. C. Holland, *Phys. Rev.* **136**, A575 (1964). These authors comment on the sensitivity of the shear constant c_{44} to variation in the interlayer spacing. The 1.7% decrease in this spacing for CMN between 273 and 4°K could therefore be expected to change the shear velocities considerably, though hardly enough to eliminate the discrepancy between the measured velocities and specific heat discussed in Sec. III.

¹⁶ See, for example, B. Taylor, H. J. Maris, and C. Elbaum, *Phys. Rev. Letters* **23**, 416 (1969).

¹⁷ J. M. Baker and B. Bleaney, *Proc. Roy. Soc. (London)* **A245**, 156 (1958).

¹⁸ A. H. Cooke and H. J. Duffus, *Proc. Roy. Soc. (London)* **A229**, 407 (1955).

¹⁹ J. W. Culvahouse, L. Pfortmiller, and D. P. Schinke, *J. Appl. Phys.* **39**, 690 (1968).

²⁰ E. R. Muller and J. W. Tucker, *Proc. Phys. Soc. (London)* **88**, 693 (1966).

²¹ V. Roundy and D. L. Mills, *Phys. Rev. B* **1**, 3703 (1970).

²² D. L. Huber, *Phys. Letters* **20**, 230 (1966).

²³ P. V. E. McClintock, I. P. Morton, R. Orbach, and H. M. Rosenberg, *Proc. Roy. Soc. (London)* **A298**, 359 (1967).

²⁴ R. J. Elliott and J. B. Parkinson, *Proc. Phys. Soc. (London)* **92**, 1024 (1967).

²⁵ L. J. Challis, M. A. McConachie, and D. J. Williams, *Proc. Roy. Soc. (London)* **A308**, 355 (1968).

²⁶ P. V. E. McClintock and H. M. Rosenberg, *Proc. Roy. Soc. (London)* **A302**, 419 (1968).

²⁷ R. T. Harley, P. V. E. McClintock, and H. M. Rosenberg, *Phys. Letters* **28A**, 469 (1969).

²⁸ G. T. Fox, M. W. Wolfmeyer, J. R. Dillinger, and D. L. Huber, *Phys. Rev.* **181**, 1308 (1969).

²⁹ D. Walton, *Phys. Rev. B* **1**, 1234 (1970).

³⁰ S. A. Al'tschuler, *Zh. Eksperim. i Teor. Fiz.* **28**, 38 (1955) [*Soviet Phys. JETP* **1**, 29 (1955)].

³¹ G. C. Westel, Jr., C. G. Roberts, E. L. Kitts, Jr., and P. O'Hagan, *Phys. Letters* **30A**, 35 (1969).

³² S. A. Al'tschuler, B. I. Kochelaev, and A. M. Leushin, *Usp. Fiz. Nauk* **75**, 459 (1961) [*Soviet Phys. Usp.* **4**, 880 (1962)].

³³ It is quite likely that the phonon free path for intrinsic scattering, M^{-1} , is also a function of θ . Since there is no way to evaluate this dependence, it is taken here to be isotropic.

³⁴ M. Krusius, A. C. Anderson, and B. Holmström, *Phys. Rev.* **177**, 910 (1969).

³⁵ W. H. Rauckhorst, Ph.D. thesis, University of Cincinnati, 1967 (unpublished).

³⁶ J. H. Van Vleck, *Phys. Rev.* **74**, 1168 (1948).

³⁷ A. G. Anderson, *Phys. Rev.* **115**, 883 (1959).